International Journal of Biological Macromolecules 164 (2020) 3698–3708

Contents lists available at ScienceDirect

International Journal of Biological Macromolecules

journal homepage: http://www.elsevier.com/locate/ijbiomac

The glutathione peroxidase family of *Theobroma cacao*: Involvement in the oxidative stress during witches' broom disease

Akyla Maria Martins Alves [a], Sara Pereira Menezes Reis [a], Karina Peres Gramacho [b], Fabienne Micheli [a,c,*]

[a] Universidade Estadual de Santa Cruz (UESC), Departamento de Ciências Biológicas (DCB), Centro de Biotecnologia e Genética (CBG), Rodovia Ilhéus-Itabuna, km 16, 45662-900 Ilhéus, BA, Brazil
[b] Cocoa Research Center, CEPLAC/CEPEC, 45600-970 Itabuna, BA, Brazil
[c] CIRAD, UMR AGAP, F-34398 Montpellier, France

ARTICLE INFO

Article history:
Received 9 January 2020
Received in revised form 26 May 2020
Accepted 28 August 2020
Available online 31 August 2020

Keywords:
Moniliophthora perniciosa
Programmed cell death
Gene expression

ABSTRACT

The glutathione peroxidases (GPXs) are enzymes which are part of the cell antioxidant system inhibiting the ROS-induced damages of membranes and proteins. In cacao (*Theobroma cacao* L.) genome, five *GPX* genes were identified. Cysteine insertion codons (UGU) were found in *TcPHGPX*, *TcGPX2*, *TcGPX4*, *TcGPX6* and tryptophan insertion codon (UGG) in *TcGPX8*. Multiple alignments revealed conserved domains between TcGPXs and other plants and human GPXs. Homology modeling was performed using the *Populus trichocarpa* GPX5 structure as template, and the molecular modeling showed that TcGPXs have affinity with selenometionine in their active site. *In silico* analysis of the *TcGPXs* promoter region revealed the presence of conserved *cis*-elements related to biotic stresses and hormone responsiveness. The expression analysis of *TcGPXs* in cacao plantlet meristems infected by *M. perniciosa* showed that *TcGPXs* are most expressed in susceptible variety than in resistant one, mainly in disease stages in which oxidative stress and programmed cell death occurred. This data, associated with phylogenetic and location analysis suggested that *TcGPXs* may play a role in protecting cells from oxidative stress as a try of disease progression reduction. To our knowledge, this is the first study of the overall GPX family from *T. cacao*.

1. Introduction

Theobroma cacao L. (cacao) is a plant endemic to the rainforests of South America [1] and is grown mainly for the production of cocoa liquor, cocoa butter, and cocoa powder for the chocolate industry [2]. However, cocoa production has been severely damaged by diseases caused by fungi and oomycete [1,3]. In Brazil, the witches' broom disease caused drastic economic and social changes in the affected areas [4,5]. This disease is caused by the *Moniliophthora perniciosa* basidiomycete that presents two distinct development phases: a biotrophic phase characterized by a monokaryotic and intercellular mycelium, and a necrotrophic phase characterized by a dikaryotic and intracellular mycelium [6,7]. In the transition from biotrophic to necrotrophic fungal phase, the plant showed significant accumulation of calcium oxalate crystals and H_2O_2, as well as events of programmed cell death (PCD) [6,8]. The accumulation of calcium oxalate causes the production of reactive oxygen species (ROS) and therefore the PCD. In cacao plants susceptible to *M. perniciosa*, the PCD occurs initially as a defense mechanism and then is deflected by the fungus for its own benefit, allowing sporulation and further propagation [6]. The transition from the biotrophic to the necrotrophic phase is facilitated by the presence of several compounds, genes, and proteins that induce PCD [8,9]. In cacao-*M. perniciosa* interaction cDNA library and/or in the cacao genome, several genes potentially related to PCD (possibly involved in its enhancement or inhibition), such as the glutathione peroxidase (GPX; EC 1.11.1.9) were found [10,11].

GPXs were first discovered in mammals and are enzymes that are part of the cell antioxidant system, inhibiting the ROS-induced damage of cell membrane and proteins [12]. GPXs reduce H_2O_2 to water and lipid hydroperoxides to their corresponding alcohols using reduced glutathione (GSH) as substrate [13]. All mammalian GPXs contain a selenocysteine (SeCys also referred to as the 21st protein amino acid) residue instead of a Cys residue [13–15]. The SeCys is encoded by an opal (TGA) stop codon, which is recognized by a special transfer RNA (tRNA); the incorporation of SeCys occurs when the mRNA contains a distinct hairpin mRNA sequence downstream of the UGA codon called SeCys insertion sequence (SECIS) [15,16]. It is admitted that yeast and plants do not incorporate SeCys and, therefore, do not have any selenoproteins [15]. However, some few studies revealed that plant kingdom may also contain selenoproteins: is has been shown that in *Chlamydomonas reinhardtii*, the GPX cDNA contained an internal TGA codon in frame to the ATG [17–19], in *Aloe vera*, native protein

* Corresponding author at: Rodovia Ilhéus-Itabuna km16, 45662-900 Ilhéus, BA, Brazil.
E-mail addresses: karina@cepec.gov.br (K. Peres Gramacho), fabienne.micheli@cirad.fr (F. Micheli).

https://doi.org/10.1016/j.ijbiomac.2020.08.222
0141-8130/

purification associated to atomic absorption revealed a molecular complex of four GPX subunits, each one containing one atom of selenium in its structure [20], and that in cranberry, the mitochondrial genome contained two copies of selenocysteine insertion sequence element (SECIS) and tRNA-SeCys [21]. It has been shown that the incorporation of SeCys rather than Cys in the active site of the GPX confers better redox activity to these enzymes [16]. In animals, and even more in plants, only little information about the GPX activity regulation is available. In animals, it has been suggested a GPX regulation at mRNA, protein and/or activity level by selenium supply, SECIS-associating factors, but also by some selenium-independent regulator; this regulation may also vary according to the GPX sequence [22]. Some studies also pointed out the role of selenium as cofactor of GPX activity [23,24]. Finally, it has also been shown the physical interaction between the human GPX1 and selenium-binding protein 1 (SBP1) – which is not a selenoprotein but is able to bind selenium covalently – associated to an inverse regulation of the two corresponding genes [25–27]. The mechanism by which SBP1 and GPX1 regulate each other remains unclear, but a competition for selenium available in the cell has been suggested as a possible mechanism of inverse regulation [28]. Altogether, these data suggested a possible physical interaction between GPX and selenium as possible element of activity regulation. In plants, selenium is absorbed from the soil in the form of selenate ($SeO4^{2-}$) or selenite ($SeO3^{2-}$) that are both toxic, and are used to synthesize SeCys and selenomethionine (SeMet) which are further converted to volatile dimethyl(*di*)selenide (DM(*D*)Se) [16]. Therefore, SeMet is one of the most abundant and metabolically important forms of selenium in plant, that could be also associated to plant selenium detoxification mechanism [16].

GPX gene expression has been related with cell protection in various stress conditions such as pathogenic attack, salt treatment, and mechanical stimulation [29]. Interestingly, in humans, the *GPX1* gene was associated to several diseases, including cancer due to disease risk-associated alleles [25,28,30]. Several studies have also reported that HsGPX1 proteins were involved in cell cycle regulation, inhibiting apoptosis that allows tumor progression [25,31,32]. For these reasons, the putative inhibitory potential of PCD associated with the ability to reduce H_2O_2 and lipid hydroperoxides makes GPXs important for understanding the cacao-*M. perniciosa* pathosystem. Here, we identified and analyzed *in silico* and *in vitro* five GPX sequences from *T. cacao*. TcGPX proteins did not contain SeCys in their primary sequence but interact with SeMet. Expression analysis of *TcGPX* genes during the cacao-*M. perniciosa* interaction showed a higher expression in susceptible cacao plants than in the resistant ones, mainly in disease stages in which oxidative stress and PCD occurred. This data, associated with phylogenetic and location analysis suggested that *TcGPXs* may play a role in protecting cells from oxidative stress, and in inhibiting PCD as a try of disease progression reduction. Moreover, the *TcGPX* expression may be regulated by several hormone pathways known to be involved in the witches' broom disease development, as indicated by the *TcGPX* promoter analysis. To our knowledge, this is the first study of the overall GPX family from *T. cacao*.

2. Methods

2.1. In silico analysis of TcGPXs

A *GPX* cDNA was identified in a library of *T. cacao* meristem (genotype TSH1188) infected by *M. perniciosa* [10]. A search in the CocoaGenDB database [11] through local alignment with BLASTn and BLASTp [33] using the *GPX* cDNA [10] allowed the identification of five homologous sequences named *TcPHGPX*, *TcGPX2*, *TcGPX4*, *TcGPX6* and *TcGPX8* according to the nomenclature and numeration of the cocoa genome (Supplementary material 1). The complete sequences of the genes and corresponding proteins were obtained from the CocoaGenDB database. The proteins were analyzed using InterProScan [34] and their classification validated by the presence of the GPX domain codes. The MCScanX tool [35] was used to identify possible duplications of the *TcGPX* genes in the cacao genome. The prediction of theoretical isoelectric point (pI) and molecular weight (MW) was obtained using the Expasy Molecular Biology Server (www.expasy.org). The conserved domain and family protein were analyzed using the Pfam program [36]. Post-translational events were predicted using the NetPhos 2.0 Server to identify putative sites of phosphorylation (Ser/Thr/Tyr) [37] and NetNGlyc 1.0 Server [38] to identify putative sites of N-glycosylation. Predictions of subcellular localization were conducted with the programs TargetP [39] and PSORT [40]. Signal peptide presence was analyzed using the SignalP 4.0 Server [41]. Homologous sequences to TcGPXs were searched using BLAST [33] on the National Center for Biotechnology Information (NCBI) and plants and mammals sequences showing the highest homology levels (> 79%) were selected. Multiple sequence alignment of these sequences was performed with the ClustalW2 software [42], and an unrooted phylogenetic tree was built using the neighbour joining method with the ClustalW2, with 1000 bootstraps [42] and MEGA 6 [43] programs. The search for regulatory sequences of the *TcGPXs* gene was performed in the CocoaGenDB database [11]. A region of 1500 bp upstream the UTR was identified and selected for *cis*-element analysis. The presence of the *cis*-regulatory elements in the promoter regions of the *TcGPX* genes was analyzed using the plantCARE (sphinx.rug.ac.be:8080/PlantCARE/cgi/index.html) software [44].

2.2. Molecular modeling and docking analysis

The prediction of the three-dimensional (3-D) models of the TcGPXs proteins was obtained using the Swiss-Model server and the Automated Protein Homology-modeling, which relies on the high similarity of target-template [45]. The crystal structure of poplar (*Populus trichocarpa*) glutathione peroxidase (PtGPX5; Protein Data Bank code: 2p5q) was used as the template to build the 3-D models of TcGPXs, because of its high identity with TcGPXs (>79%), high coverage of protein sequences and high resolution (2.0 Å). The stereochemical quality of the models was evaluated using the Procheck [46] and Anolea programs [47]. The 3-D model visualization was obtained using the PyMol (The PyMOL Molecular Graphics System, Version 1.5.0.4 Schrödinger, LLC.) and Discovery Studio 4.0. The docking analysis between TcGPXs and SeMet was performed using the AutoDockTools 1.5.6 [48]. SeMet 2D structure was found in PubChem databases (http://pubchem.ncbi.nlm.nih.gov). The 2D structure of this compound was copied into Similies and saved in PDB format using the Marvin program. The ligand and receiver structures were saved in pqbqt format to be used in docking calculations. AutoDock Vina was used to perform Docking Scoring for the complex formed by the receptor - ligand [49]. The reports of each calculation were analyzed for the energy (Kcal / Mol) values of affinity for each binder conformation in its respective complex. The Discovery Studio program was used to verify the ideal complex.

2.3. Plant material

Plant material was obtained as previously described [50]. Seeds of *T. cacao* genotypes Catongo (susceptible to *M. perniciosa*) and TSH1188 (resistant to *M. perniciosa*) were germinated and grown at CEPLAC/CEPEC (Ilhéus, Bahia, Brazil) greenhouses. Twenty to thirty days after germination, the apical meristems of the plantlets were inoculated by the droplet method [51] with a basidiospore suspension of *M. perniciosa* (inoculum from isolate 4145 maintained in the CEPLAC/CEPEC phytopathological *M. perniciosa* collection under number 921 of the WFCC; http://www.wfcc.info/index.php/collections/display). After inoculation, the plantlets were kept for 24 h at 25 ± 2 °C and 100% humidity. Rate of disease fixation based on presence/absence of symptoms [52] in each genotype, was evaluated 60 days after inoculation (dai); disease rate was 45% and 80% for TSH1188 and

Catongo, respectively. Moreover, the presence of *M. perniciosa* in the plant material was checked by semi-quantitative RT-PCR using specific *M. perniciosa* actin primers [53]; both genotypes presented fungus incidence (data not shown) coherent with previous data obtained in the same conditions of plant culture and inoculation [7]. During the overall experiment, plant development and presence/absence of symptoms were carefully checked and compared to previous disease pattern established by our research group [7]. Apical meristems were harvested at 24, 48 and 72 h after inoculation (hai), and 8, 15, 30, 45, 60 and 90 dai. Non-inoculated plants (controls) were kept and harvested under the same conditions at 24 and 72 hai, and 30 and 90 dai. Samples were collected at the same time of day (*i.e.* time of the inoculation) to avoid possible fluctuation due to circadian rhythm. For each genotype and at each harvesting time (for inoculated and non-inoculated plants), 20 samples were collected (1 sample = 1 apical meristem of 1 cacao plantlet). The 20 samples collected from one genotype at one harvesting time were pooled; thus 9 inoculated and 5 non inoculated (control) samples were immediately frozen in liquid nitrogen and stored at −80 °C until use. Pooling samples before RNA extraction has the advantage of reducing the variation caused by biological replication and sample handling [54].

2.4. Reverse transcription quantitative PCR analysis

Samples were ground on liquid nitrogen until obtaining a fine powder. Total RNA was extracted from powdered samples using the RNAqueous Kit® (Ambion) according to the manufacturer's instructions, with modifications as previously described [50]. The RNA quality and quantity were checked using the Nanodrop 2000 spectrophotometer (Thermo Scientific). The synthesis of the first cDNA strand was carried out using Revertaid Fisrt Strand cDNA Synthesis Kit according to the manufacturer's instructions (Thermo Scientific). For the qPCR analysis, two cacao endogenous reference genes were used: the malate dehydrogenase (MDH) and β-actin (ACT), previously identified as *T. cacao* housekeeping genes [55] and tested in our experimental conditions (same plant material, same equipment) [50]. Specific primers and amplified regions containing different size, melting temperature, GC content and GC/AT ratio were defined to avoid cross-reaction between genes from cacao *GPX* family (Supplementary material 2). The expression analysis of *TcPHGPX* and *TcGPX2* was performed using standard settings of the ABI PRISM 7500 and Sequence Detection System (SDS) software, version 1.6.3 (Applied Biosystems).

The qPCR reaction consisted of 10 ng/μl of cDNA, 1 μM of each primer from reference or targets genes (Supplementary material 2) and 11 μl of Power SYBR Green Master Mix (Applied Biosystems) in a total volume of 22 μl. Cycling conditions were: 50 °C for 2 min then 95 °C for 10 min, followed by 40 cycles at 95 °C for 15 s, 60 °C for 1 min and 72 °C for 30 s. To verify that each primer pair produced only a single PCR product, a dissociation analysis was carried out from 60 °C to 95 °C and analyzed with the Dissociation Curve 1.0 program (Applied Biosystems). The expression analysis of *TcGPXs* in meristems of cacao plantlets inoculated or not with *M. perniciosa*, was obtained by RT-qPCR using 3 experimental replicates. The relative expression was obtained using the comparative Ct method ($2^{-\Delta\Delta Ct}$) that considered: i) MDH and ACT as endogenous reference genes (average of expression values from both genes); and ii) non-inoculated (control) plants (average of expression values of each *TcGPX* gene in 5 control samples harvested as described above) as calibrator - for this reason the relative expression value of the control (= non-inoculated plants) is always 1.0. Statistical analysis was made using the SASM-Agri software [56] which tested the experiments as a completely randomized design. *t*-test and *F*-test (ANOVA) were applied with a critical value of 0.01. The Scott-Knott ($P \leq 0.01$) test was employed for mean separation when F-values were significant.

3. Results

3.1. In silico analysis of GPX family of T. cacao

In silico analysis on CocoaGenDB revealed the presence of five sequences encoding one *TcPHGPx* and four *TcGPXs* (*TcGPX2*, *TcGPX4*, *TcGPX6* and *TcGPX8*) (Fig. 1). *TcGPX* genes were located on four different chromosomes (chromosome 1/*TcGPX4*, chromosome 3/*TcGPX6* and *TcGPX8*, chromosome 9/*TcPHGPX* and chromosome 5/*TcGPX2*; Fig. 1A). No duplication events were found for any of the *TcGPXs* (data not shown). *TcGPX* genes were 2222 to 4805 bp in length (*TcGPX6* and *TcGPX4*, respectively; Fig. 1A), all contained 6 exons and 5 introns (Fig. 1A), and had ORF from 516 to 789 bp (*TcGPX4* and *TcGPX2*, respectively; Table 1). *TcGPXs* encoded proteins from 171 to 262 amino acids (TcGPX4 and TcGPX2, respectively; Table 1), with molecular weight comprised between 19,175.9 and 29,708.3 Da (TcGPX4 and TcGPX2, respectively; Table 1), and putative pI from 5.27 to 9.14 (TcGPX8 and TcGPX4, respectively; Table 1). All TcGPXs showed putative phosphorylation (from 7 for TcGPX4 to 22 for TcGPX6) and glycosylation (from 1 for TcPHGPX and TcGPX8 to 3 for TcGPX4 and TcGPX6) sites (Table 1). The TcPGXs were predicted to be located in chloroplast (TcPHGPX and TcGPX6), to be secreted (TcGPX2), or did not present any defined subcellular localization (unknown for TcGPX4 and TcGPX8; Table 1). The *TcGPXs* mature RNA showed the initiation codes (AUG) and cysteine insertion codons (UGU) in *TcPHGPX*, *TcGPX2*, *TcGPX4*, *TcGPX6* and the tryptophan insertion codon (UGG) in *TcGPX8* (Fig. 1B). All TcGPXs showed at least one conserved GSH domain (Fig. 1C). TcGPX family showed a cysteine instead of selenocysteine on the active site of TcPHGX, TcGPX2, TcGPX4 and TcGPX6 and a tryptophan on the active site of TcGPH8 instead of a selenocysteine (Fig. 1C). The alignment of TcGPXs sequence using the BLASTP tool revealed high identity with GPXs from other organisms (plant and mammals) and allowed the identification of the conserved region containing a conserved cysteine residue in plants and SeCys is mammals (Supplementary material 3). The full-length amino acid sequences of plants and mammalian of GPXs available in the databases were used to build an unrooted phylogenetic tree (Supplementary material 4). Plant and mammalian GPXs were separated and formed two distinct branches in the tree (Fig. 2). The five TcGPXs have close phylogenetic relationship with members of the same classification in other plant species (Fig. 2). *In silico* analysis of the TcGPXs promoter region revealed the presence of several conserved *cis*-elements characteristic of different plant species (Table 2). Elements recognized by the family of WRKY transcription factors (W box) were identified in all *TcGPX* promoters, and defense and stress responsiveness elements (TC-rich repeats) were identified in *TcPHGPX*, *TcGPX2*, *TcGPX6* and *TcGPX8* (Table 2). Elements related to response to abiotic stress or external stimuli anaerobic induction (ARE), light responsiveness (BOX4), drought-inducibility (MBS), Low-temperature responsiveness (LTR) were also found (Table 2). Finally, several *cis*-elements related to hormone signaling were found such as abscisic acid responsiveness (ABRE), gibberellin-responsive element (GARE-motif), MeJA-responsiveness (TGACG-motif), salicylic acid responsiveness, (TCA-element) and auxin-responsive element (TGA-element) (Table 2).

3.2. Homology modeling of GPXs and docking analysis

The alignment of the PtGPX5 (3-D template) amino acid sequence showed 63.92%, 69.03%, 59.17%, 75.15% and 84.02% with TcPHGPXs, TcGPX2, TcGPX4, TcGPX6, TcGPX8, respectively (Fig. 3A). The structural modeling of TcPHGPX, TcGPX4 and TcGPX6 showed 8 α-helices and 6 β-strands (Fig. 3B, D and E) while TcGPX2 showed 6 α-helices and, 6 β-strands (Fig. 3C) and TcGPX8 7 α-helices and 6 β-strands (Fig. 3F). The Ramachandran plots showed that 100% of the amino acids of the TcGPXs models were located in the most favored regions (Supplementary material 5). The catalytic site of TcPHGPX, TcGPX2, TcGPX4, and TcGPx6 contained the conserved cysteine (Cys_{114}, Cys_{75}, Cys_{44}, and

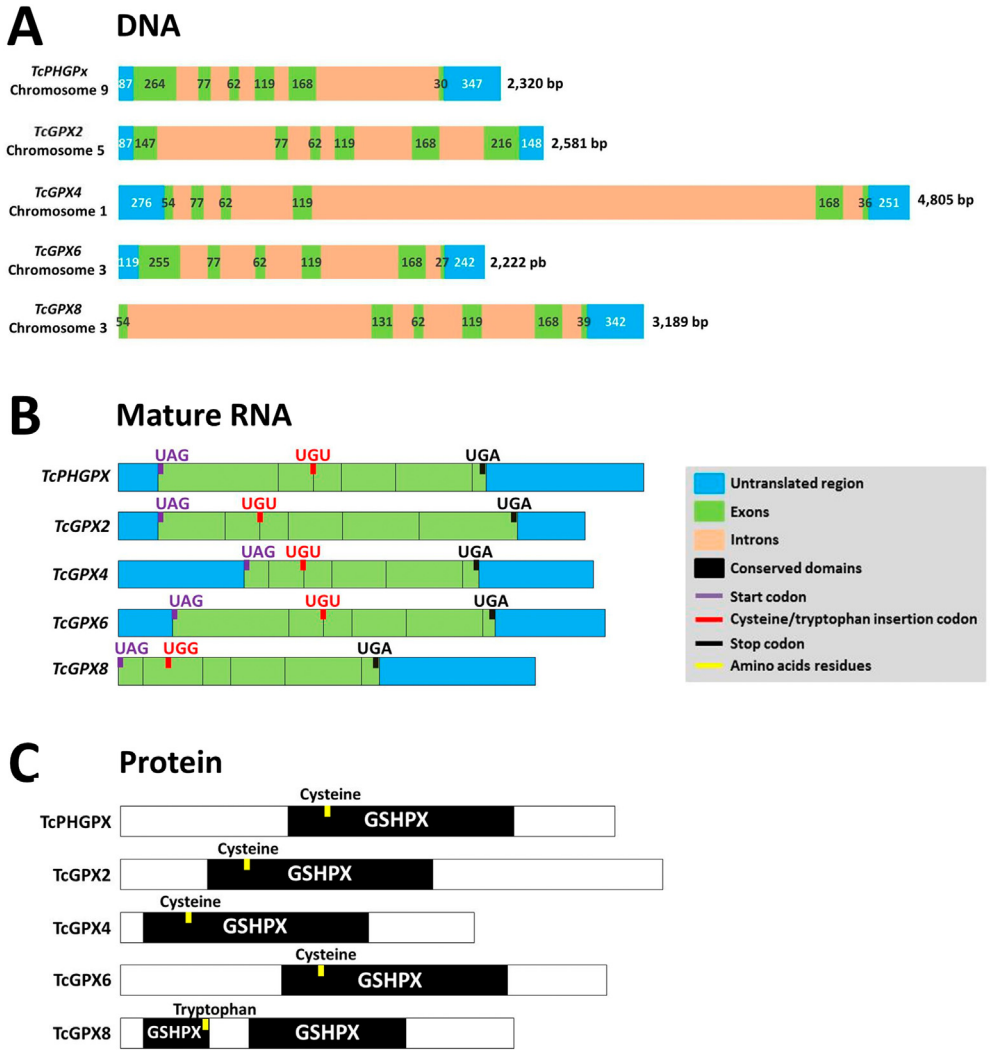

Fig. 1. Schematic illustration of the genes, mature RNA and proteins of the GPX family from *Theobroma cacao*. **A.** DNA sequences of GPX family. Untranslated regions, exons and introns are indicated by turquoise, green and salmon squares, respectively. **B.** Mature RNAs from the *TcGPX* genes. Untranslated regions and exons are indicated by turquoise and green squares, respectively. Purple lines represent the initiation codons (AUG), red lines indicate the cysteine insertion codons (UGU) in *PHGPX*, *GPX2*, *GPX4*, *GPX6* and the tryptophan insertion codon (UGG) in *GPX8*, and black lines indicate the stop codons (UGA). **C.** TcGPX protein structure. Black squares represent the conserved GSH domain and yellow lines indicate the presence of cysteine on the active site of TcPHGX, TcGPX2, TcGPX4 and TcGPX6, and of tryptophan on the active site of TcGPX8, instead of selenocysteine.

Cys_{111}, respectively) residue (Fig. 3A, B, C, D and E). TcGPX8 contained two conserved tryptophan (W_{44}, W_{151}) residue (Fig. 3A and F). The docking between TcPHGPXs and SeMet showed conventional hydrogen bond interactions between Lys_{113}, Cys_{114}, Thr_{163} and, carbon hydrogen bond between Pro_{151} (Fig. 4A). The interaction between TcGPX4 and SeMet showed conventional hydrogen bond between Gln_{75}, Ser_{129}, Asn_{108}, Arg_{136} and, unfavorable donor-donor between Arg_{130} (Fig. 4B). The interaction between TcGPX6 and SeMet showed conventional hydrogen bond between Asp_{196}, Arg_{216}, Thr_{221} and, unfavorable donor-donor between Ala_{218} (Fig. 4C). The interaction between TcGPx8 and SeMet showed Pi-sulfur interaction between Phe_{58}, conventional hydrogen bond between Tyr_{45}, Trp_{44} and Glu_{97} and carbon hydrogen between Trp_{151} (Fig. 4D). No interaction was observed between TcGPX2 and SeMet (data not shown).

3.3. Differential expression of TcGPXs in resistant and susceptible cacao genotypes infected by M. perniciosa

The expression of the *TcPHGPX*, *TcGPX2*, *TcGPX4*, *TcGPX6*, and *TcGPX8* genes was analyzed together for each cacao genotype, *i.e.* TSH1188 (resistant to witches' broom disease) and Catongo (susceptible), infected or not (control) with *M. perniciosa* (Fig. 5A). For both genotypes and for all the harvesting points, the PCR amplification occurred at the same and unique melting temperature for each gene showing that only the corresponding gene was amplified (Supplementary material 6). When we analyzed the gene expression the according to the disease stage (time after inoculation), we verified that, in the resistant variety, the *TcPHGPX* gene did not differ significantly at 24 and 48 hai, with a small repression compared to the non-inoculated control (Fig. 5B). At 72 hai, the *TcPHGPX* gene becomes significantly more expressed than the control (Fig. 5B). At 8 and 15 dai, the expression of the *TcPHGPX* gene did not differ significantly, however, they were significantly more expressed than the control (Fig. 5B). At 30 dai, *TcPHGPX* was significantly less expressed than the control, and at 45 and 90 dai did not differ from the control (Fig. 5B). At 60 dai, the *TcPHGPX* gene was overexpressed in the resistant variety (Fig. 5B). In the resistant variety, the *TcGPX2* gene did not differ significantly from the control after 24, 48 and 72 hai, as well as after 15, 45, and 60 dai after inoculation (Fig. 5B). At 8 dai, the *TcGPX2* gene was repressed compared to the control (Fig. 5B). At 30 dai, the *TcGPX2* gene was also less expressed than the control (Fig. 5B). At 90 dai, the *TcGPX2* gene was significantly more expressed than in the non-inoculated control (Fig. 5B). The *TcGPX4* gene was only significantly more expressed than the control at 60 and 90 dai (Fig. 5B). The *TcGPX6* gene was significantly more expressed at

Table 1
Gene and protein characteristics of GPX family from *T. cacao*. nd: non determined.

Name	Predict gene data				Predict protein data					
	Identification[a]	Sequence start[a]	Sequence end[a]	ORF size (bp)	Size (aa)	Molecular weight (Da)	pI	Subcellular localization	Phosphorylation sites	Glycosylation sites
TcPHGPX	Tc09_p001340	728,482	730,367	720	239	26,477.2	9.08	Chloroplast	S_{33} S_{36} S_{40} S_{43} S_{44} S_{58} S_{70} S_{96} S_{98} S_{122} S_{153} T_{20} T_{78} T_{81}	N_{120}
TcGPX2	Tc05_p000210	101,857	104,202	789	262	29,708.3	9.11	Secretory	S_{31} S_{42} S_{57} S_{59} S_{62} S_{152} T_{47} T_{185} T_{246} Y_{44} Y_{92} Y_{147}	N_{165} N_{227}
TcGPX4	Tc01_p028750	24,070,592	24,074,869	516	171	19,175.9	9.14	nd	S_{11} S_{28} S_{121} T_{16} T_{83} Y_{52} Y_{116}	N_{50} N_{122} N_{134}
TcGPX6	Tc03_p027320	23,147,873	23,149,733	780	235	25,973.7	8.93	Chloroplast	S_{25} S_{29} S_{31} S_{32} S_{43} S_{52} S_{57} S_{63} S_{74} S_{75} S_{78} S_{95} S_{188} S_{189} S_{197} S_{225} T_{83} T_{221} Y_{118} Y_{128} Y_{166} Y_{183}	N_{12} N_{117} N_{201}
TcGPX8	Tc03_p027330	23,150,262	23,153,108	573	190	21,600.4	5.27	nd	S_{5} S_{11} S_{28} S_{50} S_{159} S_{173} S_{176} T_{16} T_{54} Y_{13} Y_{69} Y_{79} Y_{134}	N_{68}

[a] Gene identification and position as indicated in CocoaGenDB database.

30, 45, and 60 dai, with a peak expression of 60 dai, followed by a 90 dai repression (Fig. 5B). The *TcGPX8* gene was significantly more expressed than the control at 45, 60, and 90 dai. In the previous periods they were less expressed than the non-inoculated control (Fig. 5B). In the susceptible variety the *TcPHGPX* gene was overexpressed at 24 and 48 hai (Fig. 5C). At 72 hai and at 8 and 15 dai, the *Tc*PHGPX gene was differentially less expressed than the non-inoculated control (Fig. 5C). At 30 and 45 dai, the *TcPHGPX* gene did not differ significantly from the non-inoculated control (Fig. 5C). The *TcGPX2* gene was repressed within 24 hai after being overexpressed at 48 and 72 hai (Fig. 5C). At 30 dai the *TcGPX2* gene was less expressed than the control (Fig. 5C). At 24 hai, 8, 15, and 60 dai the *TcGPX4* gene did not differ from the control (Fig. 5C). At 48 and 72 hai and 90 dai *TcGPX4* was less expressed than the control (Fig. 5C). At 30 and 45 dai the *TcGPX4* gene was overexpressed (Fig. 5C). The *TcGPX6* gene was overexpressed at 24 hai and 30, 45 and 90 dai. At 48 and 72 hai and 8 and 15 dai the expression of the *TcGPX6* gene did not differ significantly from the non-inoculated control. At 60 dai the *TcGPX6* gene was significantly less expressed than the control (Fig. 5C). The *TcGPX8* gene was overexpressed at 24 hai and 30 and 45 dai (Fig. 5C). It was significantly less expressed than the control at 48 and 72 hai (Fig. 5C). At 60 and 90 dai the *TcGPX8* gene was significantly more expressed than the control (Fig. 5C).

When comparing the expression of the *TcGPX* family genes, we observed that in the resistant variety, 24 hai there was significant difference between the *TcPHGPX* and *TcGPX8* genes (Fig. 5B). At 48 hai there was no significant difference between the genes of the TcGPX family (Fig. 5B). At 72 hai *TcPHGPX* and *TcGPX6* were significantly more expressed (Fig. 5B). *TcGPx4* and *TcGPx8* did not differ significantly after 72 hai (Fig. 5B). At 8 dai *TcPHGPX* was significantly more expressed and *TcGPX2* was less expressed (Fig. 5B). At 15 dai there was no difference between the genes of the *TcGPX* family (Fig. 5B). At 30 dai *TcGPX6* was significantly more expressed, whereas *TcPHGPX* and *TcGPx2* were less expressed (Fig. 5B). At 43 dai *TcGPX6* and *TcGPX8* were significantly more expressed, respectively (Fig. 5B). After 60 dai *TcGPx6* was significantly more expressed, whereas *TcGPX2* was less expressed (Fig. 5B). At 90 dai the *TcGPX2*, *TcGPX4* and *TcGPX8* genes were significantly more expressed than the *TcPHGPX* and *TcGPX6* genes (Fig. 5B).

In the susceptible variety, after 24 hai the *TcPHGPX* gene was overexpressed and *TcGPX2* was less expressed than the control (Fig. 5C). At 48 hai *TcPHGPX* and *TcGPX2* were significantly more expressed, whereas *TcGPX4*, *TcGPX6* and *TcGPX8* were less expressed than the control (Fig. 5C). At 8 dai *TcGPX2* and *TcGPX4* did not differ from the control, whereas *TcPHGPX*, *TcGPX6* and *TcGPX8* were less

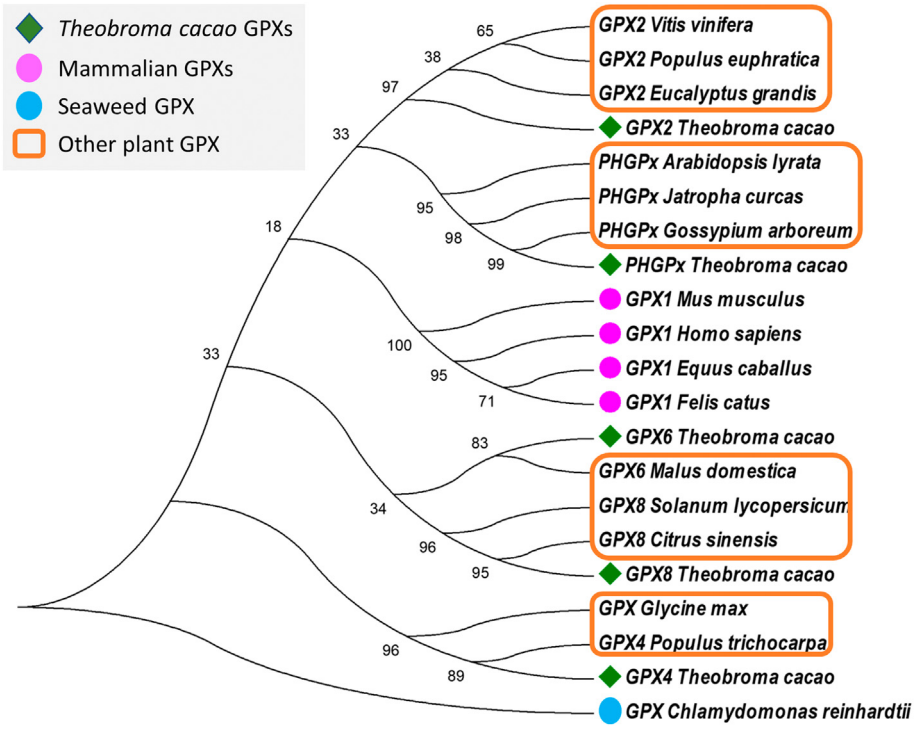

Fig. 2. Phylogenetic relationships among the nucleotide sequences of TcGPXs and other plants and mammalian GPXs. Only complete sequences were considered. The tree was constructed using the neighbour-joining method of clustalW with 1000 bootstraps. The amino acid sequences were obtained from GenBank.

Table 2
Cis-elements present in the promoter region of *T. cacao GPX* genes.

Gene	Name of *cis*-elements	Organism	Function
	ABRE	*Arabidopsis thaliana*	Abscisic acid responsiveness
	ARE	*Zea mays*	Anaerobic induction
	AT-rich	*Pisum sativum*	Maximal elicitor-mediated activation
TcPHGPX	Box 4	*Petroselinum crispum*	Light responsiveness
	MBS	*Arabidopsis thaliana*	Drought-inducibility
	TC-rich repeats	*Nicotiana tabacum*	Defense and stress responsiveness
	W box	*Arabidopsis thaliana*	WRKY transcription factors
	ABRE	*Arabidopsis thaliana*	Abscisic acid responsiveness
	GARE-motif	*Brassica oleracea*	Gibberellin-responsive element
	MBS	*Arabidopsis thaliana*	Drought-inducibility
TcGPX2	TC-rich repeats	*Nicotiana tabacum*	Defense and stress responsiveness
	W box	*Arabidopsis thaliana*	WRKY transcription factors
	Box 4	*Petroselinum crispum*	Light responsiveness
	TGACG-motif	*Hordeum vulgare*	MeJA-responsiveness
	ABRE	*Arabidopsis thaliana*	Abscisic acid responsiveness
	ARE	*Zea mays*	Anaerobic induction
	Box 4	*Petroselinum crispum*	Light responsiveness
	GARE-motif	*Brassica oleracea*	Gibberellin-responsive element
TcGPX4	MBS	*Arabidopsis thaliana*	Drought-inducibility
	P-box	*Oryza sativa*	Gibberellin-responsive element
	TCA-element	*Nicotiana tabacum*	Salicylic acid responsiveness
	TGA-element	*Brassica oleracea*	Auxin-responsive element
	W box	*Arabidopsis thaliana*	WRKY transcription factors
	ABRE	*Arabidopsis thaliana*	Abscisic acid responsiveness
	ARE	*Zea mays*	Anaerobic induction
	Box 4	*Petroselinum crispum*	Light responsiveness
	LTR	*Hordeum vulgare*	Low-temperature responsiveness
TcGPX6	TC-rich repeats	*Nicotiana tabacum*	Defense and stress responsiveness
	TGA-element	*Brassica oleracea*	Auxin-responsive element
	TGACG-motif	*Hordeum vulgare*	MeJA-responsiveness
	W box	*Arabidopsis thaliana*	WRKY transcription factors
	ABRE	*Arabidopsis thaliana*	Abscisic acid responsiveness
	ARE	*Zea mays*	Anaerobic induction
	Box 4	*Petroselinum crispum*	Light responsiveness
	AT-rich	*Pisum sativum*	Maximal elicitor-mediated activation
	MBS	*Arabidopsis thaliana*	Drought-inducibility
TcGPX8	O2-site	*Zea mays*	Zein metabolism regulation
	TATC-box	*Oryza sativa*	Gibberellin-responsiveness
	TC-rich repeats	*Nicotiana tabacum*	Defense and stress responsiveness
	TCA-element	*Brassica oleracea*	Salicylic acid responsiveness
	TGA-element	*Brassica oleracea*	Auxin-responsive element
	W box	*Arabidopsis thaliana*	WRKY transcription factors

expressed than the control (Fig. 5C). After 30 dai the *TcGPX4* and *TcGPX8* genes were overexpressed and *TcGPX2* was less expressed than the control (Fig. 5C). At 45 dai *TcGPX4*, *TcGPX6* and *TcGPX8* were significantly more expressed than *TcPHGPX* and *TcGPX2* (Fig. 5C). After 60 dai the *TcPHGPX*, *TcGPX2,* and *TcGPX6* genes were less expressed than the control. The *TcGPX4* and *TcGPX8* genes did not differ from the control (Fig. 5C). At 90 dai the *TcGPX6* gene was significantly more expressed and the *TcGPX4* gene was less expressed than the non-inoculated control (Fig. 5C).

4. Discussion

4.1. TcGPX protein family did not contain SeCys but interacted in silico with SeMet

Here, we characterized five GPXs (TcPHGPX, TcGPX2, TcGPX4, TcGPX6 and TcGPX8) sequences from *T. cacao* (Fig. 1). All the TcGPX protein, except TcGPX8, contained a conserved GSHPX domain with conserved Cys residues (Fig. 1C), which are important for the protein function [13]. Even if it has been related in few studies the possible existence of selenoproteins in plants [17,20,21], our results corroborate the difference already observed in most of the cases between GPXs from plants and animals: the active site of plant GPXs contains a Cys while the one of animal GPXs contains SeCys [57]. In the case of TcGPX8, the Cys residue was substituted by a tryptophan residue within the GSHPX domain. Although tryptophan is an amino acid with antioxidant activity [58] and could act as a hydrogen donor [59], it differs greatly from the chemical structure of cysteine. It could be suggested that TcGPX8 may be a non-functional GPX due to some sequence truncation or mutation. On the other hand, here, we showed that TcGPXs (except TcGPX2) are able to bind *in silico* the SeMet chemical element (Fig. 4). Some plant GPXs may have increased activity or be selenodependent even without the presence of the UGA codon for incorporation of SeCys [22,28]. The possibility of GPXs having increased activity when interacting with selenium compounds is due to the fact that selenium serves as a GPX cofactor [23,24]. Thus, as suggested here by molecular docking assays, the TcGPXs may present PCD inhibition and antioxidant activities if they were associated with selenium compounds (Fig. 4).

4.2. TcGPXs are ubiquitous protein potentially involved in cell death inhibition

All the TcGPX proteins contained multiple predicted phosphorylation and glycosylation sites (Table 1), which are ubiquitous mechanism for the temporal and spatial regulation of proteins involved in almost every cellular process [60]. The TcGPXs family showed an ubiquitous subcellular localization (Table 1) including chloroplast location (TcHGPX and TcGPX6) where these proteins may use GSH or thioredoxin as a reducing agent to reduce H_2O_2, organic hydroperoxide,

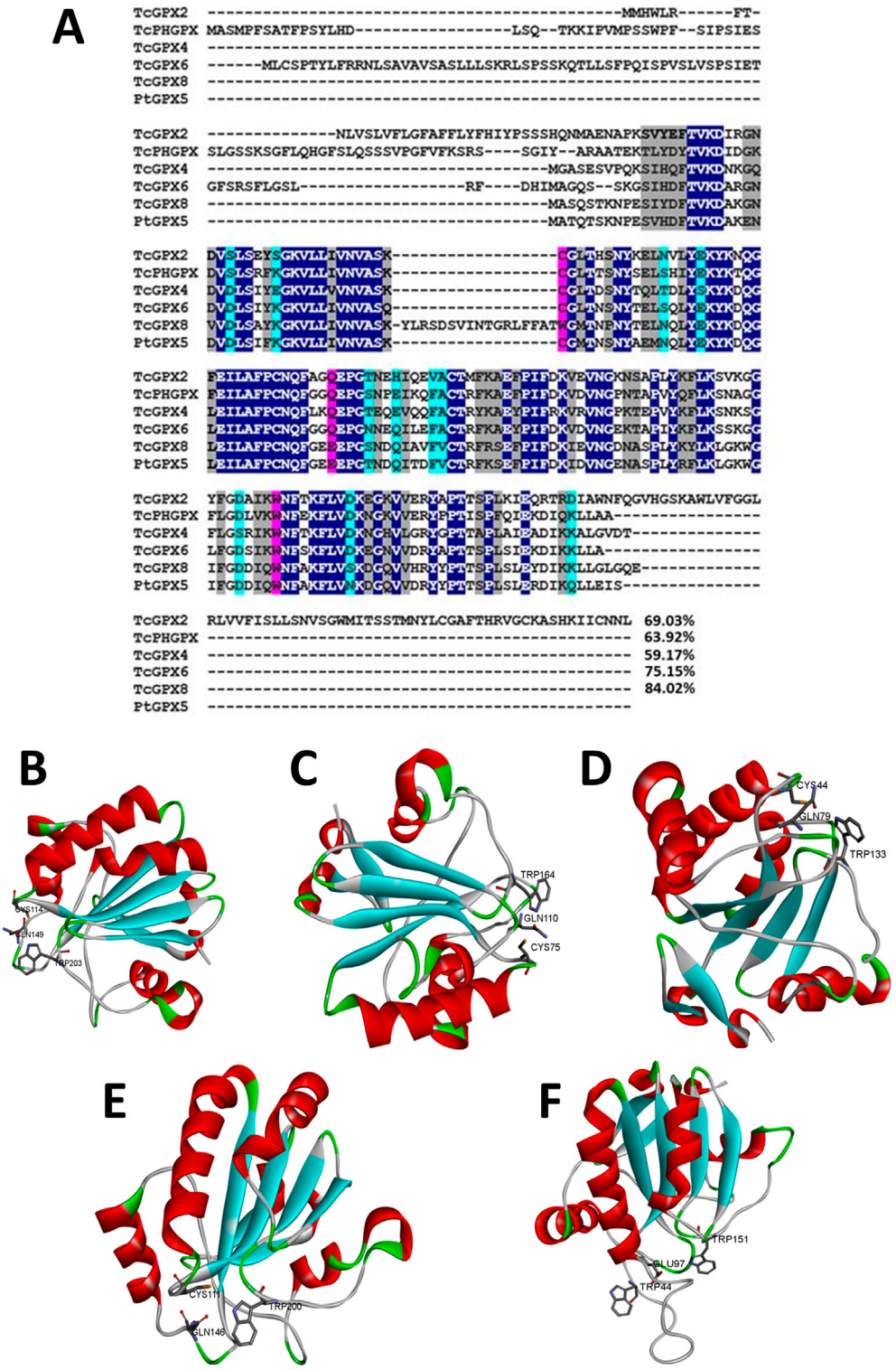

Fig. 3. Tridimensional structure of TcPHGPX, TcGPX2, TcGPX4, TcGPX6, and TcGPX8 obtained by homology modeling with PtGPx5 from *Populus trichocarpa* (2P5R.pdb). **A.** Alignment of the TcGPX with PtGPx5. Conserved substitutions, identical amino acids, semi-conserved substitutions and catalytic triad are indicated in grey, dark blue, light blue and purple, respectively. **B.** Secondary structure of TcPHGPX. **C.** Secondary structure of TcGPX2. **D.** Secondary structure of TcGPX4. **E.** Secondary structure of TcGPX6. **F.** Secondary structure of TcGPX8. **B**—**F.** The catalytic triad of each TcGPX is represented by a solvent surface.

and lipid hydroperoxides [61]. Furthermore, in Arabidopsis it has been shown that chloroplastic GPXs play a role in cross talk between photooxidative stress and immune responses [61,62]. The phylogenetic analysis of TcGPXs with different GPX from plants and animals showed that they were very conserved inclusive for each sub-group of GPX, *i.e.* PHGPXs *vs* GPXs (Fig. 2). The sequence and structure conservation of TcGPXs also suggests a conservation of function as indicated by other authors [13]. In mammal signal transduction pathways, it has been suggested that PHGPx functions as an anti-apoptotic agent in mitochondrial death signaling [63]. The antioxidant GPX enzymes eliminate ROS and reduce H_2O_2 [64,65] and in human, are known to be inhibitors of apoptosis [66]. Functional studies of *Lycopersicon esculentum* PHGPX (*LePHGPx*)

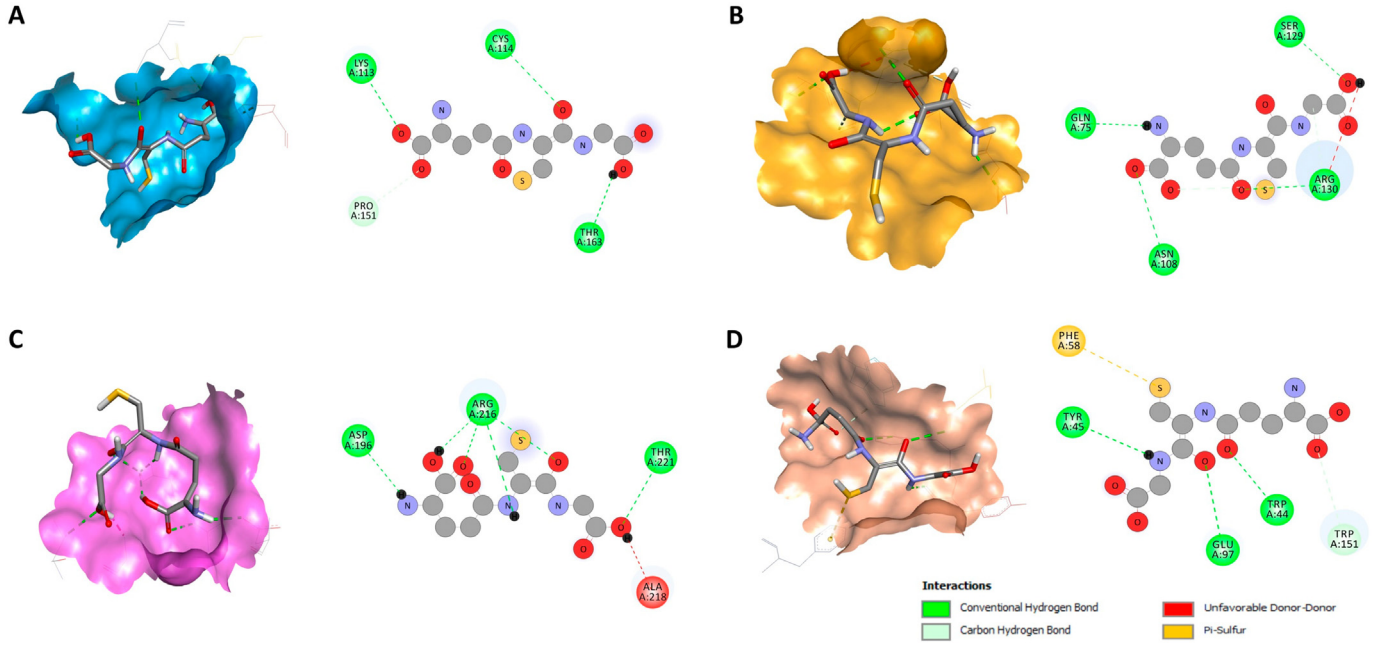

Fig. 4. Docking between TcGPXs and selenomethionine (SeMet). **A.** Interaction between TcPHGPX (blue) and SeMet. **B.** Interaction between TcGPX4 (orange) and SeMet. **C.** Interaction between TcGPX6 (pink) and SeMet. **D.** Interaction between TcGPX8 (salmon) and SeMet.

showed that this gene acted as a cytoprotector in yeast, preventing Bax, hydrogen peroxide, and heat stress induced cell death, but also protected tobacco leaves from salt and heat stress and suppressed the apoptotic like features when expressed transiently in this plant [67]. In addition, stable expression of LePHGPx in tobacco afforded protection against the necrotrophic fungus *Botrytis cinerea* [67].

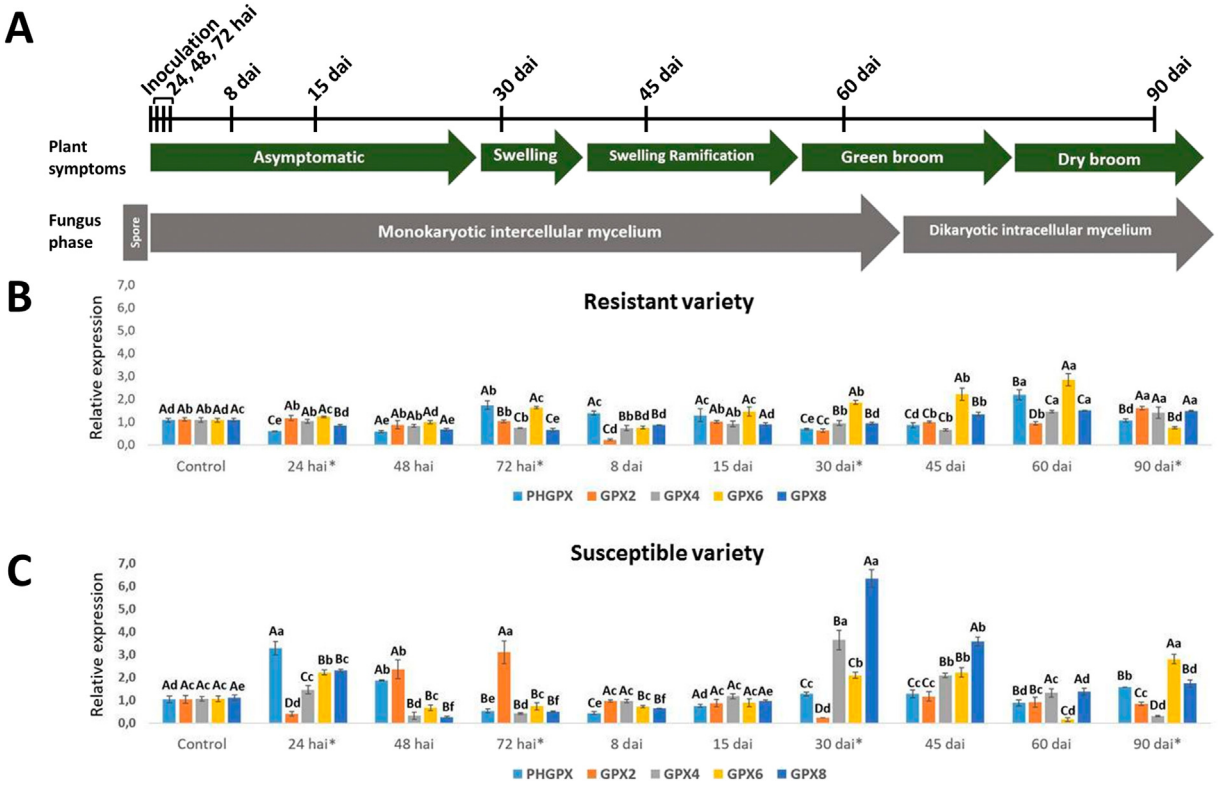

Fig. 5. Relative expression of *TcPHGPX*, *TcGPX2*, *TcGPX4*, *TcGPX6*, and *TcGPX8* in cacao meristems inoculated or not (control) with *M. perniciosa*. **A.** Representation of plant symptoms and fungus phase during the infection time course in Catongo genotypes. The harvesting times of inoculated plants are indicated on the top of the figure. **B.** Relative expression observed in TSH1188. **C.** Relative expression observed in Catongo. (*) indicates harvesting times of non-inoculated (control) plants. The control, used as calibrator (for this reason is always 1), corresponds to the average of the expression values of each *TcGPX* in 5 non-inoculated samples in each genotype (see also Methods section). Different letters indicate significant statistical difference between samples by the Scott-Knott test p($p \leq 0.01$). *t*-test was applied with a critical value of 0.01: upper case letters correspond to statistics between each of the genes on different harvesting times for each genotype while lower case letters correspond to statistics among the genes for each harvesting time. hai: hours after inoculation; dai: days after inoculation.

4.3. TcGPXs may be involved in PCD reduction during T. cacao – M. perniciosa interaction

The expression analysis of *TcGPX* genes by RT-qPCR in cacao plant meristems infected by *M. perniciosa* showed that these genes are significantly more expressed in the susceptible variety than in the resistant one (Fig. 5B and C). Moreover, considering the susceptible variety, *TcGPX* are most expressed during asymptomatic and green broom stages (Fig. 5). During dry broom phase *TcGPx6* is significantly more expressed than the other genes in the susceptible variety (Fig. 5C). *TcGPx2* is significantly more expressed in swelling phase in susceptible variety (Fig. 5A e C). In previous works, it has been showed that calcium oxalate crystal amount and H_2O_2 levels in the two cacao varieties present distinct temporal and genotype dependent patterns [8]. Susceptible variety accumulated more CaOx crystals than the resistant one [8,9], the dissolution of these crystals occurred in the asymptomatic and in the final stages of the disease in the resistant and the susceptible variety, respectively [8,9]. Considering the role of the GPXs in the antioxidant system inhibiting the ROS-induced damages, it could be suggested that in the susceptible cacao genotype infected with *M. perniciosa*, *TcGPXs* may play a role in protecting cells from oxidative stress and trying reducing the progression of the disease by inhibiting PCD. Moreover, the increase of *TcPHGPX* expression in susceptible variety in the initial stage of witches' broom disease may be related to protection against pathogens observed in other pathosystems [67].

The *TcGPX* expression regulation was led by promoter regions, which contained several *cis*-elements related to biotic (WRKY transcription factors) and abiotic stress (low-temperature responsiveness) besides to hormone signaling such abscisic acid, gibberellin, methyljasmonate-responsiveness, salicylic acid and, auxin-responsive element (Table 2). Most of these hormones are involved in witches' broom disease development [10,68–70]. Several genes related to plant hormone signaling were altered in cacao plants in response to *M. perniciosa* infection, such ethylene-responsive element, ABA-responsive protein, auxin-responsive protein, jasmonic acid 2, and brassinosteroid signaling positive regulator [10]. Gibberellin-responsive, ethylene biosynthesis as well as auxin-responsive genes were also previously identified as up-regulated in green broom [70]. Is has been suggested that the up-regulation of auxin-responsive genes in infected cacao plants is a consequence of the biosynthesis of this hormone by *M. perniciosa* [68–70]. In various plant pathogens, the production of auxin has been correlated to the reduction of the plant defenses mediated by salicylic acid, and consequently to the pathogenicity and to the biotrophic stage development [68,70].

5. Conclusion

Here we showed the first *in silico* and *in vitro* analysis of the GPX family from cacao. Five TcGPXs sequences were analyzed at nucleotide and protein levels, and showed that the TcGPX proteins did not contain SeCys in their primary sequence but interacts *in silico* with SeMet as element participating of the TcGPX activity. This characteristic, associated to phylogenetic and location analyses, suggested the participation of TcGPX in cell death inhibition. Finally, the *TcGPX* genes were more expressed in susceptible cacao plants infected by *M. perniciosa* than in the resistant ones, mainly in the early disease and in the green broom stages, suggesting that *TcGPXs* may play a role in protecting cells from oxidative stress, in inhibiting PCD as a try of disease progression reduction. This expression may be regulated by several hormone pathways known to be involved in the witches' broom disease development.

Availability of supporting data

The data sets supporting the results of this article are included within the article and its additional files.

Abbreviations

ACT: actin
dai: days after inoculation
GPX: glutathione peroxidase
GSH: reduced glutathione
hai: hour after inoculation
pI: isoeletric point
MDH: malate dehydrogenase
MW: molecular weight
ORF: open reading frame
PCD: programmed cell death
PHGPX: phospholipid hydroperoxide glutathione peroxidase
UTR: untranslated regions

CRediT authorship contribution statement

AMMA was responsible for the execution of the all the experimental steps; AMMA, SPMR, and FM analyzed and discussed the data; AMMA and FM wrote the manuscript; SPMR gave support in qPCR experiment; KPG was responsible for plant material production and inoculation with *M. perniciosa*; FM and AMMA were responsible for the conception and design of the experiments; FM was responsible for the financial support of the research and for the advising of AMMA and SPMR.

Declaration of competing interest

No conflicts of interest to declare.

Acknowledgements

The work of AMMA was supported by the Fundação de Amparo à Pesquisa do Estado da Bahia (FAPESB). The work of SPMR was supported by the Coordenação de Aperfeiçoamento de Pessoal de Nível Superior (CAPES). KPG and FM received a Productivity grant from the Conselho Nacional de Desenvolvimento Científico e Tecnológico (CNPq). This research was supported by the FAPESB project (DTE0038/2013) coordinated by FM. The authors thank Francisca Feitosa Jucá (UESC/Ceplac) and Louise Araújo Sousa (Ceplac) for technical help in plant inoculation experiments. The authors thank Raner José Santana Silva (UESC) for advising in modeling, and Dr. Janisete Gomes da Silva Miller (UESC) for correcting English language. This work was developed in the frame of the International Consortium in Advanced Biology (CIBA; https://www.ciba-network.org/).

Appendix A. Supplementary data

Supplementary data to this article can be found online at https://doi.org/10.1016/j.ijbiomac.2020.08.222.

References

[1] G.A.R. Wood, R.A. Lass, Cocoa, Fourth Edition ed. Blackwell Science Ltd, 1985.
[2] E.O. Afoakwa, A. Paterson, M. Fowler, A. Ryan, Flavor formation and character in cocoa and chocolate: a critical review, Crit. Rev. Food Sci. Nutr. 48 (9) (2008) 840–857.
[3] F. Micheli, M. Guiltinan, K.P. Gramacho, M.J. Wilkinson, A.V.d.O. Figueira, J.C.d.M. Cascardo, S. Maximova, C. Lanaud, Chapter 3 - functional genomics of cacao, in: K. Jean-Claude, D. Michel (Eds.), Advances in Botanical Research, Academic Press 2010, pp. 119–177.
[4] H.M. Rocha, R.A.C. Miranda, R.B. Sgrillo, R.A. Setubal, S.A. Rudgard, A.C. M., A. T., Witches' broom in Bahia, Brazil, Disease and Management in Cocoa: Comparative Epidemiology of Witches' Broom, Chapman and Hall, London 1993, pp. 189–200.
[5] L.W. Meinhardt, J. Rincones, B.A. Bailey, M.C. Aime, G.W. Griffith, D. Zhang, G.A. Pereira, *Moniliophthora perniciosa*, the causal agent of witches' broom disease of cacao: what's new from this old foe? Mol. Plant Pathol. 9 (5) (2008) 577–588.
[6] O. Garcia, J.A. Macedo, R. Tiburcio, G. Zaparoli, J. Rincones, L.M. Bittencourt, G.O. Ceita, F. Micheli, A. Gesteira, A.C. Mariano, M.A. Schiavinato, F.J. Medrano, L.W. Meinhardt, G.A. Pereira, J.C. Cascardo, Characterization of necrosis and ethylene-

inducing proteins (NEP) in the basidiomycete *Moniliophthora perniciosa*, the causal agent of witches' broom in *Theobroma cacao*, Mycol. Res. 111 (Pt 4) (2007) 443–455.
[7] K. Sena, L. Alemanno, K.P. Gramacho, The infection process of *Moniliophthora perniciosa* in cacao, Plant Pathol. (2014) 1272–1281.
[8] C.V. Dias, J.S. Mendes, A.C. dos Santos, C.P. Pirovani, A. da Silva Gesteira, F. Micheli, K.P. Gramacho, J. Hammerstone, P. Mazzafera, J.C. de Mattos Cascardo, Hydrogen peroxide formation in cacao tissues infected by the hemibiotrophic fungus *Moniliophthora perniciosa*, Plant Physiol. Biochem. 49 (8) (2011) 917–922.
[9] G. de Oliveira Ceita, J.N.A. Macêdo, T.B. Santos, L. Alemanno, A. da Silva Gesteira, F. Micheli, A.C. Mariano, K.P. Gramacho, D. da Costa Silva, L. Meinhardt, P. Mazzafera, G.A.G. Pereira, J.C. de Mattos Cascardo, Involvement of calcium oxalate degradation during programmed cell death in *Theobroma cacao* tissues triggered by the hemibiotrophic fungus *Moniliophthora perniciosa*, Plant Sci. 173 (2) (2007) 106–117.
[10] A.S. Gesteira, F. Micheli, N. Carels, A. Da Silva, K. Gramacho, I. Schuster, J. Macedo, G. Pereira, J. Cascardo, Comparative analysis of expressed genes from cacao meristems infected by *Moniliophthora perniciosa*, Ann. Bot. 100 (1) (2007) 129–140.
[11] X. Argout, J. Salse, J.-M. Aury, M.J. Guiltinan, G. Droc, J. Gouzy, M. Allegre, C. Chaparro, T. Legavre, S.N. Maximova, M. Abrouk, F. Murat, O. Fouet, J. Poulain, M. Ruiz, Y. Roguet, M. Rodier-Goud, J.F. Barbosa-Neto, F. Sabot, D. Kudrna, J.S.S. Ammiraju, S.C. Schuster, J.E. Carlson, E. Sallet, T. Schiex, A. Dievart, M. Kramer, L. Gelley, Z. Shi, A. Berard, C. Viot, M. Boccara, A.M. Risterucci, V. Guignon, X. Sabau, M.J. Axtell, Z. Ma, Y. Zhang, S. Brown, M. Bourge, W. Golser, X. Song, D. Clement, R. Rivallan, M. Tahi, J.M. Akaza, B. Pitollat, K. Gramacho, A. D'Hont, D. Brunel, D. Infante, I. Kebe, P. Costet, R. Wing, W.R. McCombie, E. Guiderdoni, F. Quetier, O. Panaud, P. Wincker, S. Bocs, C. Lanaud, The genome of *Theobroma cacao*, Nat. Genet. 43 (2011) 101–108.
[12] D. Trachootham, J. Alexandre, P. Huang, Targeting cancer cells by ROS-mediated mechanisms: a radical therapeutic approach? Nat. Rev. Drug Discov. 8 (2009) 579.
[13] R. Margis, C. Dunand, F.K. Teixeira, M. Margis-Pinheiro, Glutathione peroxidase family – an evolutionary overview, FEBS J. 275 (15) (2008) 3959–3970.
[14] S. Herbette, P. Roeckel-Drevet, J.R. Drevet, Seleno-independent glutathione peroxidases. More than simple antioxidant scavengers, FEBS J 274 (9) (2007) 2163–2180.
[15] E. Zoidis, I. Seremelis, N. Kontopoulos, G.P. Danezis, Selenium-dependent antioxidant enzymes: actions and properties of Selenoproteins, Antioxidants (Basel) 7 (5) (2018) 66.
[16] M. Schiavon, E.A. Pilon-Smits, The fascinating facets of plant selenium accumulation - biochemistry, physiology, evolution and ecology, New Phytol. 213 (4) (2017) 1582–1596.
[17] L.-H. Fu, X.-F. Wang, Y. Eyal, Y.-M. She, L.J. Donald, K.G. Standing, G. Ben-Hayyim, A selenoprotein in the plant kingdom: mass spectrometry confirms that an opal codon (UGA) encodes selenocysteine in chlamydomonas reinhardtii glutathione peroxidase, J. Biol. Chem. 277 (29) (2002) 25983–25991.
[18] S.V. Novoselov, M. Rao, N.V. Onoshko, H. Zhi, G.V. Kryukov, Y. Xiang, D.P. Weeks, D.L. Hatfield, V.N. Gladyshev, Selenoproteins and selenocysteine insertion system in the model plant cell system, *Chlamydomonas reinhardtii*, The EMBO Journal 21 (14) (2002) 3681–3693.
[19] D.Y. Lee, O. Fiehn, High quality metabolomic data for Chlamydomonas reinhardtii, Plant Methods 4 (2008) 7.
[20] F. Sabeh, T. Wright, S.J. Norton, Purification and characterization of a glutathione peroxidase from the aloe vera plant, Enzyme Protein 47 (1993) 92–98.
[21] D. Fajardo, B. Schlautman, S. Steffan, J. Polashock, N. Vorsa, J. Zalapa, The American cranberry mitochondrial genome reveals the presence of selenocysteine (tRNA-Sec and SECIS) insertion machinery in land plants, Gene 536 (2) (2014) 336–343.
[22] X.G. Lei, W.H. Cheng, J.P. McClung, Metabolic regulation and function of glutathione peroxidase-1, Annu. Rev. Nutr. 27 (2007) 41–61.
[23] S. Chan, B. Gerson, S. Subramaniam, The role of copper, molybdenum, selenium, and zinc in nutrition and health, Clin. Lab. Med. 18 (4) (1998) 673–685.
[24] M. Puccinelli, F. Malorgio, B. Pezzarossa, Selenium enrichment of horticultural crops, Molecules 22 (6) (2017).
[25] W. Fang, M.L. Goldberg, N.M. Pohl, X. Bi, C. Tong, B. Xiong, T.J. Koh, A.M. Diamond, W. Yang, Functional and physical interaction between the selenium-binding protein 1 (SBP1) and the glutathione peroxidase 1 selenoprotein, Carcinogenesis 31 (8) (2010) 1360–1366.
[26] M. Schott, M.M. de Jel, J.C. Engelmann, P. Renner, E.K. Geissler, A.K. Bosserhoff, S. Kuphal, Selenium-binding protein 1 is down-regulated in malignant melanoma, Oncotarget 9 (12) (2018) 10445–10456.
[27] F. Schild, S. Kieffer-Jaquinod, A. Palencia, D. Cobessi, G. Sarret, C. Zubieta, A. Jourdain, R. Dumas, V. Forge, D. Testemale, J. Bourguignon, V. Hugouvieux, Biochemical and biophysical characterization of the selenium-binding and reducing site in Arabidopsis thaliana homologue to mammals selenium-binding protein 1, J. Biol. Chem. 289 (46) (2014) 31765–31776.
[28] E. Ansong, W. Yang, A.M. Diamond, Molecular cross-talk between members of distinct families of selenium containing proteins, Mol. Nutr. Food Res. 58 (1) (2014) 117–123.
[29] W.-J. Li, H. Feng, J.-H. Fan, R.-Q. Zhang, N.-M. Zhao, J.-Y. Liu, Molecular cloning and expression of a phospholipid hydroperoxide glutathione peroxidase homolog in Oryza sativa1, Biochimica et Biophysica Acta (BBA) - Gene Structure and Expression 1493 (1–2) (2000) 225–230.
[30] A. Jerome-Morais, M.E. Wright, R. Liu, W. Yang, M.I. Jackson, G.F. Combs, A.M. Diamond, Inverse association between glutathione peroxidase activity and both selenium binding protein 1 levels and Gleason score in human prostate tissue, Prostate 72 (9) (2012) 1006–1012.
[31] C. Huang, G. Ding, C. Gu, J. Zhou, M. Kuang, Y. Ji, Y. He, T. Kondo, J. Fan, Decreased selenium-binding protein 1 enhances glutathione peroxidase 1 activity and downregulates HIF-1α to promote hepatocellular carcinoma invasiveness, Clin. Cancer Res. 18 (11) (2012) 3042–3053.
[32] J.-Y. Jeong, J.-R. Zhou, C. Gao, L. Feldman, A.J. Sytkowski, Human selenium binding protein-1 (hSP56) is a negative regulator of HIF-1α and suppresses the malignant characteristics of prostate cancer cells, BMB Rep. 47 (7) (2014) 411–416.
[33] S.F. Altschul, T.L. Madden, A.A. Schaffer, J. Zhang, Z. Zhang, W. Miller, D.J. Lipman, Gapped BLAST and PSI-BLAST: a new generation of protein database search programs, Nucleic Acids Res. 25 (17) (1997) 3389–3402.
[34] E. Quevillon, V. Silventoinen, S. Pillai, N. Harte, N. Mulder, R. Apweiler, R. Lopez, InterProScan: protein domains identifier, Nucleic Acids Res. 33 (Suppl. 2) (2005) W116–W120.
[35] Y. Wang, H. Tang, J.D. DeBarry, X. Tan, J. Li, X. Wang, T.-h. Lee, H. Jin, B. Marler, H. Guo, J.C. Kissinger, A.H. Paterson, MCScanX: a toolkit for detection and evolutionary analysis of gene synteny and collinearity, Nucleic Acids Res. 40 (7) (2012) e49.
[36] S. El-Gebali, J. Mistry, A. Bateman, S.R. Eddy, A. Luciani, S.C. Potter, M. Qureshi, L.J. Richardson, G.A. Salazar, A. Smart, E.L.L. Sonnhammer, L. Hirsh, L. Paladin, D. Piovesan, S.C.E. Tosatto, R.D. Finn, The Pfam protein families database in 2019, Nucleic Acids Res. 47 (D1) (2019) D427–D432.
[37] N. Blom, S. Gammeltoft, S. Brunak, Sequence and structure-based prediction of eukaryotic protein phosphorylation sites, J. Mol. Biol. 294 (5) (1999) 1351–1362.
[38] R. Gupta, S. Brunak, Prediction of glycosylation across the human proteome and the correlation to protein function, Pac. Symp. Biocomput. (2002) 310–322.
[39] O. Emanuelsson, S. Brunak, G. von Heijne, H. Nielsen, Locating proteins in the cell using TargetP, SignalP and related tools, Nat. Protocols 2 (4) (2007) 953–971.
[40] K. Nakai, P. Horton, PSORT: a program for detecting sorting signals in proteins and predicting their subcellular localization, Trends Biochem. Sci. 24 (1) (1999) 34–35.
[41] T.N. Petersen, S. Brunak, G. von Heijne, H. Nielsen, SignalP 4.0: discriminating signal peptides from transmembrane regions, Nat Meth 8 (10) (2011) 785–786.
[42] M.A. Larkin, G. Blackshields, N.P. Brown, R. Chenna, P.A. McGettigan, H. McWilliam, F. Valentin, I.M. Wallace, A. Wilm, R. Lopez, J.D. Thompson, T.J. Gibson, D.G. Higgins, Clustal W and Clustal X version 2.0, Bioinformatics 23 (21) (2007) 2947–2948.
[43] K. Tamura, G. Stecher, D. Peterson, A. Filipski, S. Kumar, MEGA6: molecular evolutionary genetics analysis version 6.0, Mol. Biol. Evol. 30 (12) (2013) 2725–2729.
[44] M. Lescot, P. Déhais, G. Thijs, K. Marchal, Y. Moreau, Y. Van de Peer, P. Rouzé, S. Rombauts, PlantCARE, a database of plant *cis*-acting regulatory elements and a portal to tools for in silico analysis of promoter sequences, Nucleic Acids Res. 30 (1) (2002) 325–327.
[45] K. Arnold, L. Bordoli, J. Kopp, T. Schwede, The SWISS-MODEL workspace: a web-based environment for protein structure homology modelling, Bioinformatics 22 (2) (2006) 195–201.
[46] R.A. Laskowski, M.W. MacArthur, D.S. Moss, J.M. Thornton, PROCHECK: a program to check the stereochemical quality of protein structures, J. Appl. Crystallogr. 26 (2) (1993) 283–291.
[47] F. Melo, E. Feytmans, Assessing protein structures with a non-local atomic interaction energy, J. Mol. Biol. 277 (5) (1998) 1141–1152.
[48] M. Sanner, A.J. Olson, J.C. Spehner, Reduced surface: an efficient way to compute molecular surfaces, Biopolymers 38 (3) (1996) 305–320.
[49] O. Trott, A.J. Olson, AutoDock Vina: improving the speed and accuracy of docking with a new scoring function, efficient optimization and multithreading, J. Comput. Chem. 31 (2) (2010) 455–461.
[50] S. Pereira Menezes, E. de Andrade Silva, E. Matos Lima, A. Oliveira de Sousa, B. Silva Andrade, L. Santos Lima Lemos, K. Peres Gramacho, A. da Silva Gesteira, C. Pirovani, F. Micheli, The pathogenesis-related protein PR-4b from *Theobroma cacao* presents RNase activity, Ca^{2+} and Mg^{2+} dependent-DNase activity and antifungal action on *Moniliophthora perniciosa*, BMC Plant Biol. 14(1) (2014) 1–17.
[51] G. Frias, L. Purdy, R. Schmidt, An inoculation method for evaluating resistance of cacao to *Crinipellis perniciosa*, Plant Dis. 79 (1995) 787–791.
[52] S. Silva, K. Matsuoka, Histologia da interação *Crinipellis perniciosa* em cacaueiros suscetível e resistente à vassoura de bruxa, Fitopatol. Bras. 24 (1999) 54–59.
[53] R.X. Santos, S.C.O. Melo, J.C.M. Cascardo, M. Brendel, C. Pungartnik, Carbon source-dependent variation of acquired mutagen resistance of *Moniliophthora perniciosa*: similarities in natural and artificial systems, Fungal Genet. Biol. 45 (6) (2008) 851–860.
[54] S. Duplessis, P.-E. Courty, D. Tagu, F. Martin, Transcript patterns associated with ectomycorrhiza development in *Eucalyptus globulus* and *Pisolithus microcarpus*, New Phytol. 165 (2) (2004) 599–611.
[55] T.T. Pinheiro, C.G. Litholdo Jr., M.L. Sereno, G.A. Leal Jr., P.S.B. Albuquerque, A. Figueira, Establishing references for gene expression analyses by RT-qPCR in *Theobroma cacao* tissues, Genet. Mol. Res. 10 (4) (2012) 3291–3305.
[56] M.G. Canteri, R.A. Althaus, J.S. das Virgens Filho, E.A. Giglioti, C.V. Godoy, SASM-AGRI - Sistema para analise e separação de médias em experimentos agricolas pelos métodos Scott-Knott, Tukey a Duncan, Revista Brasileira de Agrocomputação 1 (2) (2001) 18–24.
[57] T.C. Stadtman, Selenocysteine, Annu. Rev. Biochem. 65 (1) (1996) 83–100.
[58] S. Katayama, Y. Mine, Antioxidative activity of amino acids on tissue oxidative stress in human intestinal epithelial cell model, J. Agric. Food Chem. 55 (21) (2007) 8458–8464.
[59] R.J. Elias, D.J. McClements, E.A. Decker, Antioxidant activity of cysteine, tryptophan, and methionine residues in continuous phase beta-lactoglobulin in oil-in-water emulsions, J. Agric. Food Chem. 53 (26) (2005) 10248–10253.
[60] Samuel M. Pearlman, Z. Serber, James E. Ferrell Jr, A mechanism for the evolution of phosphorylation sites, Cell 147 (4) (2011) 934–946.
[61] C.-Z. Zhai, L. Zhao, L.-J. Yin, M. Chen, Q.-Y. Wang, L.-C. Li, Z.-S. Xu, Y.-Z. Ma, Two wheat glutathione peroxidase genes whose products are located in chloroplasts improve salt and H(2)O(2) tolerances in Arabidopsis, PLoS One 8 (10) (2013), e73989.

[62] C.C.C. Chang, I. Slesak, L. Jordá, A. Sotnikov, M. Melzer, Z. Miszalski, P.M. Mullineaux, J.E. Parker, B. Karpinska, S. Karpinski, Arabidopsis chloroplastic glutathione peroxidases play a role in cross talk between photooxidative stress and immune responses, Plant Physiol. 150 (2) (2009) 670–683.

[63] K. Nomura, H. Imai, T. Koumura, T. Kobayashi, Y. Nakagawa, Mitochondrial phospholipid hydroperoxide glutathione peroxidase inhibits the release of cytochrome c from mitochondria by suppressing the peroxidation of cardiolipin in hypoglycaemia-induced apoptosis, The Biochemical journal 351 (Pt 1) (2000) 183–193.

[64] M.A.R. Milla, A. Maurer, A.R. Huete, J.P. Gustafson, Glutathione peroxidase genes in Arabidopsis are ubiquitous and regulated by abiotic stresses through diverse signaling pathways, Plant J. 36 (5) (2003) 602–615.

[65] Z. Faltin, D. Holland, M. Velcheva, M. Tsapovetsky, P. Roeckel-Drevet, A.K. Handa, M. Abu-Abied, M. Friedman-Einat, Y. Eshdat, A. Perl, Glutathione peroxidase regulation of reactive oxygen species level is crucial for in vitro plant differentiation, Plant Cell Physiol. 51 (7) (2010) 1151–1162.

[66] R. Franco, J.A. Cidlowski, Apoptosis and glutathione: beyond an antioxidant, Cell Death Differ. 16 (10) (2009) 1303–1314.

[67] S. Chen, Z. Vaghchhipawala, W. Li, H. Asard, M.B. Dickman, Tomato phospholipid hydroperoxide glutathione peroxidase inhibits cell death induced by Bax and oxidative stresses in yeast and plants, Plant Physiol. 135 (3) (2004) 1630–1641.

[68] A. Kilaru, B.A. Bailey, K.H. Hasenstein, *Moniliophthora perniciosa* produces hormones and alters endogenous auxin and salicylic acid in infected cocoa leaves, FEMS Microbiol. Lett. 274 (2) (2007) 238–244.

[69] F.C. Chaves, T.J. Gianfagna, Necrotrophic phase of Moniliophthora perniciosa causes salicylic acid accumulation in infected stems of cacao, Physiol. Mol. Plant Pathol. 69 (1–3) (2006) 104–108.

[70] P.J.P.L. Teixeira, D.P.d.T. Thomazella, O. Reis, P.F.V. do Prado, M.C.S. do Rio, G.L. Fiorin, J. José, G.G.L. Costa, V.A. Negri, J.M.C. Mondego, P. Mieczkowski, G.A.G. Pereira, High-resolution transcript profiling of the atypical biotrophic interaction between Theobroma cacao and the fungal pathogen Moniliophthora perniciosa, Plant Cell 26 (11) (2014) 4245–4269.